

THESIS FOR THE DEGREE OF LICENTIATE OF ENGINEERING
IN THERMO AND FLUID DYNAMICS

Numerical Simulations of the Urban Microclimate

PATRICIA VANKY

Department of Mechanics and Maritime Sciences
CHALMERS UNIVERSITY OF TECHNOLOGY
Gothenburg, Sweden, 2023

Numerical Simulations of the Urban Microclimate

PATRICIA VANKY

© Patricia Vanky, 2023

Thesis for the degree of Licentiate of Engineering No. 2023:01
Department of Mechanics and Maritime Sciences
Division of Fluid Dynamics
Chalmers University of Technology
SE-412 96 Göteborg,
Sweden
Phone: +46(0)31 772 1000

Printed by Chalmers Digitaltryck,
Gothenburg, Sweden 2023.

Numerical Simulations of the Urban Microclimate

PATRICIA VANKY

Department of Mechanics and Maritime Sciences

Chalmers University of Technology

ABSTRACT

As global urbanization is accelerating and the majority of the world's population continues to reside in cities, sustainable urban development is becoming increasingly crucial. Evaluation of the urban microclimate is a vital aspect of planning sustainable cities, as it can significantly impact on the health and comfort of urban residents. Computational Fluid Dynamics is a cost-effective and flexible tool to predict microclimate conditions, although often not utilized in the urban planning process until the final stages of a project due to complex pre-processing. The current practice of urban planning also often involves simulating different physical phenomena in separate tools, making it difficult to understand the interaction. This thesis presents the potential of the numerical immersed boundary framework IBOFlow as a tool for urban planners to evaluate the urban microclimate at the early stages of the design processes. The complex and time-consuming pre-processing of urban regions is eliminated using automatically generated Cartesian octree grid meshes where the complex geometries are represented by the immersed boundary methodology. The framework is validated for wind using wind tunnel experiments and compared to a commercially used software to show the importance of including the complex local terrain to generate realistic results. Finally, initial results of the heat simulations are covered to visualize the idea of IBOFlow as a means to simulate the urban microclimate at large, including all necessary physics.

Keywords

CFD modelling, Experimental validation, Immersed Boundary, Urban microclimate, Wind comfort

ACKNOWLEDGEMENTS

First and foremost, I am deeply grateful to my main supervisor, Gaetano Sardina, for providing me with this opportunity and for always being available to discuss potential issues and new approaches, helping me develop as a researcher. I also extend my sincere thanks to my co-supervisors, Andreas Mark and Angela Sasic Kalagasidis, for their valuable insights and constructive feedback. I will always be thankful for how flexible and supportive you have all been when circumstances change.

I am also grateful to the Urban Environmental Quality (UEQ) project, funded by the Swedish Research Council for Sustainable Development (Formas) under grants 2019-01169 and 2019-01885, for enabling me to conduct this research. Thank you to my colleges in the project, Franziska Hunger, Marie Haeger-Eugensson, Joaquim Tarraso and Marco Adelfio for fruitful discussions and invaluable input from different points-of-view. Additionally, I would like to thank the Digital Twin Cities Centre, supported by Sweden's Innovation Agency Vinnova under Grant No. 2019-00041, for their collaboration. The computations were enabled by resources provided by the Swedish National Infrastructure for Computing (SNIC) at C3SE partially funded by the Swedish Research Council through grant agreement no. 2018-05973.

Furthermore, I would like to thank my colleges at the Department of Mechanics and Maritime Sciences, Division of Fluid Dynamics at Chalmers University of Technology for making it a joy to come to work everyday.

Last but not least, I would like to thank my husband for everything that you are! Thank you for always helping when you can help and distracting when I need to refocus. Thanks to my family for your unconditional love and support. And to my unborn child, thanks for being so cooperative these last few months, this could have been much harder than it has been.

Patricia Vanky
Gothenburg, February 2023

NOMENCLATURE

Abbreviations

BPG	Best Practice Guidelines
CFD	Computational Fluid Dynamics
CPU	Central Processing Unit
DNS	Direct Numerical Simulation
FCC	Fraunhofer Chalmers Research Centre
GPU	Graphical Processing Unit
HPC2N	High Performance Computing Center North
HTC	Heat Transfer Coefficient
IBOFlow	Immersed Boundary Octree Flow Solver
MISKAM	Microscale Climate and Dispersion Model
PET	Physiological Equivalent Temperature
PIV	Particle Image Velocimetry
SDG	Sustainable Development Goals
UHI	Urban Heat Island
UN	United Nations
UTCI	Universal Thermal Climate Index
WBGT	Wet-Bulb Globe Temperature
LES	Large Eddy Simulation
RANS	Reynolds-Averaged Navier-Stokes
SIMPLEC	Semi-Implicit Method for Pressure Linked Equations Consistent

Greek Letters

ε	Rate of dissipation	$\text{m}^2 \text{s}^{-3}$
μ	Dynamic viscosity	$\text{kg m}^{-1} \text{s}^{-1}$
ω	Specific rate of dissipation	s^{-1}
ρ	Density	kg m^{-3}

Roman Letters

C_μ	constant	
f	Numerical source	$\text{kg m}^{-2} \text{s}^{-2}$
g^2	Turbulence time scale	s^{-1}
k	Turbulence kinetic energy	$\text{m}^2 \text{s}^{-2}$
k_s	Sand grain roughness height	m
p	Pressure	$\text{kg m}^{-1} \text{s}^{-2}$
t	Time	s
x	Position	m
z_0	Aerodynamic roughness length	m
u	Velocity	m s^{-2}

Superscripts and Subscripts

$\langle \rangle_{bc}$	Boundary cell node
$\langle \rangle_i$	x-component
$\langle \rangle^{ib}$	Immersed Boundary position

$\langle \rangle_j$
 $\langle \rangle_m$

y-component
Mirrored node

LIST OF PUBLICATIONS

This thesis is based on the following publications:

- Paper A** P. Vanky, A. Mark, F. Hunger, M. Haeger-Eugensson, J. Tarraso, M. Adelfio, A. Sasic Kalagasidis, G. Sardina, Addressing wind comfort in an urban area using an immersed boundary framework, *Technische Mechanik-European Journal of Engineering Mechanics*, accepted awaiting publication.
- Paper B** P. Vanky, A. Mark, F. Hunger, M. Haeger-Eugensson, J. Tarraso, M. Adelfio, A. Sasic Kalagasidis, G. Sardina, Evaluation of Wind in Urban Regions with Complex Local Topography Using an Immersed Boundary Framework, *Submitted for journal publication*, under review.

OTHER PUBLICATIONS

The following publications were published during my PhD studies. However, they are not appended to this thesis, due to contents overlapping that of appended publications.

Paper I P. Vanky, A. Mark, F. Hunger, M. Haeger-Eugensson, J. Tarraso, M. Adelfio, A. Sasic Kalagasidis, G. Sardina, Validation of an immersed boundary framework for urban flows, *Proc. Conference on Modelling Fluid Flow (CMFF'22)*, Budapest, Hungary (2022) pp. 237-245, CMFF22-044.

CONTENTS

Abstract	i
Acknowledgement	iii
Nomenclature	v
List of Publications	vii
I Extended Summary	1
1 Introduction	3
1.1 Background	3
1.2 Aim	4
2 Urban microclimate	7
2.1 Urban heat islands	7
2.1.1 Urban heat dome	9
2.2 Man-made building materials	9
2.3 Vegetation and water bodies	10
2.4 Urban furniture	11
2.5 Perceived urban comfort	12
2.5.1 Wind comfort criteria	12
2.5.2 Heat comfort indices	13
3 Numerical simulations of urban regions	15
3.1 Current practice	15
3.1.1 Simulation application	15
3.1.2 Set-up process	16
3.1.3 Numerical schemes and models	16
3.1.4 Best Practice Guidelines	17
3.1.5 Lacking in current practice	18
3.2 IBOFlow	19
3.2.1 Immersed Boundary Method	19
3.2.1.1 Mirrored immersed boundary condition	20
3.2.2 Turbulence modelling	21
3.2.3 Heat transfer modelling	22
3.2.3.1 Heat transfer in fluids	22
3.2.3.2 Coupled fluid and solid heat transfer	22
3.2.4 Wall functions	23
4 Selected Results	25
4.1 Wind tunnel validation	25
4.2 Urban scale simulations	27
4.2.1 Wind comfort	29

4.3 Heat simulations	29
5 Summary of papers	33
5.1 Paper A	33
5.2 Paper B	34
6 Concluding remarks	35
6.1 Summary	35
6.2 Future work	36
Bibliography	37
II Appended Papers	45

Part I

Extended Summary

Chapter 1

Introduction

1.1 Background

Since 2008, the majority of the world population has been living in cities, and with the acceleration of global urbanization, it has been projected that by 2050 close to 70% of humanity will reside in urban areas [1]. This trend highlights the importance of addressing sustainable urban development globally. This is reflected in the inclusion of a stand-alone goal on cities and urban development in the United Nations's (UN) 2030 Agenda, Sustainable Development Goal (SDG) 11, "make cities and human settlements inclusive, safe, resilient and sustainable" [2]. In addition, urban related topics are acknowledged to be multifaceted and have a strong influence on other Sustainable Development Goals (such as SDGs 1, 6, 7, 8, 9, 12, 15, and 17, among others).

Wind and heat evaluation are important to consider when planning sustainable cities, as they can have significant impacts on the comfort and well-being of urban residents [3]. Wind can affect factors such as the mitigation of pollutants and the distribution of heat and moisture, which can be linked to significant physical and mental health problems among those living in urban areas [4]. Designing and planning urban environments for better wind and heat conditions can also impact residential energy consumption, for example, related to air conditioning [5].

Various methods can be utilized to assess wind and heat in city planning. One approach is to use physical models, such as wind tunnels or thermal comfort chambers, which can be used to study the wind and heat conditions in a controlled environment. These models can provide detailed data on the wind and heat conditions in an urban environment, and they can be used to test different design scenarios and assess their impacts on the wind and heat conditions [6]. However, the downside of physical models is that they tend to be costly and not flexible to changes in geometry [7].

Another approach is to use field measurements, and monitoring can be used to collect data on the wind and heat conditions in a real urban environment. This can include measurements of temperature, humidity, wind speed and direction, and other factors that can affect the wind and heat conditions [8].

However, field measurements are limited to existing built environments and specific climate conditions, which is hard to use for planning new urban regions. Nevertheless, the data gathered could be used to compare and evaluate similar regions and to gain a deeper understanding of wind and heat conditions in a specific urban setting. Therefore, the primary purpose of the data would be to validate other models. In the validation, it is important to consider the measured governing parameters may vary due to unpredictable meteorological conditions during the measurement intervals, while numerical and physical modeling tend to be more stable in their inlet conditions.

Finally, numerical simulations, such as Computational Fluid Dynamics (CFD) simulations or urban wind simulations, can be used, which can help to predict the wind and heat conditions in a specific urban environment. These simulations can study a wide range of phenomena, including the shape and orientation of the urban features, the presence of vegetation, local heat loads, and the surrounding terrain topography. There are many advantages to using CFD, such as cost, flexibility, versatility, and time which makes it an important tool for understanding the complex interactions between fluids and urban environments [9]–[11]. However, despite all advantages of using CFD, it is often not utilized in the urban planning process until the final stages of a project due to the difficulty of setting up the simulation. By this point, it is often too late to make significant changes to the design.

To summarize, the evaluation of wind and heat is a crucial aspect of city planning so that city planners and designers can better understand the wind and heat conditions in an urban environment and design urban spaces that are more livable and comfortable for urban residents. Furthermore, by considering wind and heat in the planning process at early stages, cities can create more sustainable and resilient urban environments that can better adapt to the impacts of climate change [3]–[5]. One way to make wind and heat evaluation more accessible is to use CFD, but the numerical tools require expertise today, which limits their use in practice.

1.2 Aim

Because of the technical complexity that requires specialized training and expertise to set up and interpret urban simulations, a barrier is created for urban planners who may not have a background in engineering or computer science. In addition, CFD simulations can be expensive to set up and run, although typically less than physical modelling and field measurements, which can limit their use in urban planning projects. This work aims to explore ways in which computational fluid dynamics can be made more accessible and useful for urban planners in the design and assessment of urban environments. Specifically, the work aims to cover the following points:

- Identification of the current barriers to the wider adoption of CFD in urban planning, including technical, cost, and knowledge-related issues.
- Investigate best practices and case studies of successful urban CFD

simulations to identify successful strategies and approaches.

- Develop a more accessible and user-friendly CFD tool for urban planners, including simplifying the simulation setup process, reducing simulation time and providing guidelines for general settings.

Chapter 2

Urban microclimate

By replacing the natural rural environments with urban settlements, where residential, commercial and industrial buildings, roads and other infrastructures cover most of the land area, a unique and local microclimate is formed. The urban microclimate can differ significantly from the regional climate, and it can have a significant impact on the people living in these areas [12].

One key aspect of the urban microclimate is the Urban Heat Island (UHI) effect, which is the phenomenon of higher temperatures in urban areas compared to surrounding rural areas [13], [14]. Other factors that can affect the urban microclimate include the presence of vegetation and water bodies, where the first can provide shade and evaporative cooling, which can help regulate temperature [15]. The design of the built environment, for example, the orientation of buildings, including urban furniture and the use of reflective surfaces and heat-storing materials, can also impact the urban microclimate [16]–[18].

In general, the microclimate within urban areas is a multifaceted and crucial aspect of understanding the urban environment. Therefore, urban planners and designers must consider a wide range of factors that can impact the local climate to create cities with improved microclimate, a task that presents a significant challenge and requires a holistic approach.

2.1 Urban heat islands

As mentioned, Urban Heat Islands are the phenomenon where urban areas experience higher temperatures than surrounding rural areas due to the built environment [13], [14]. A general distribution of the temperature over rural and urban regions can be seen in Fig. 2.1. There are several physical processes that contribute to the formation of urban heat islands, including the absorption and storage of heat by buildings and other structures, the reflection of heat by paved surfaces, the release of heat by industrial and transportation activities and anthropogenic heat. The first two, heat absorption and storage, as well as reflective surfaces, will be further discussed in Section 2.2. Industrial and transportation activities contribute to the formation of urban heat islands

by releasing heat into the environment by burning fossil fuels. The high concentration of industry and traffic in cities exacerbates this warming trend in urban regions.

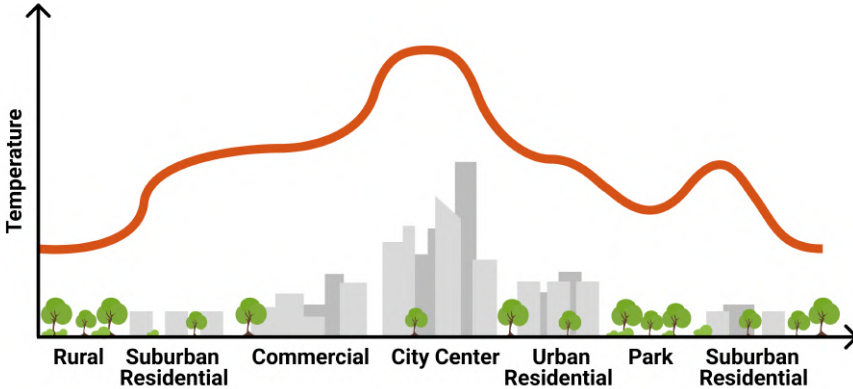


Figure 2.1: Generalized distribution of temperature over rural and urban regions

Furthermore, UHIs are characterized by their temporal nature, meaning that they are subject to changes over time, including the time of day, the time of year, and the overall weather patterns in the area. For example, studies by Oke et al. (1991) [19] as well as Kim and Baik (2002) [20] have shown that the maximum urban heat island effect is present at night and in winter when the difference between the urban and rural areas is large. It was also shown that clear weather produced stronger heat island effects, where as in periods of cloudy or rainy weather, when solar radiation is reduced, the effect was less pronounced.

The increased temperature due to UHIs is significant and can have negative consequences for both the environment and human health. For example, high temperatures can lead to an increase in energy consumption as the usage of air conditioning and other cooling measures in homes and buildings increases. This can contribute to an overall increase in greenhouse gas emissions, as the production and use of energy often involve the release of carbon dioxide and other greenhouse gases into the atmosphere [5]. Heat islands can also affect local ecosystems and wildlife. For example, higher temperatures can lead to a decline in the quality of air and water resources, which can have negative impacts on plants and animals. High temperatures can also disrupt the life cycles of certain species, as they may not be adapted to the warmer temperatures found in urban heat islands [21].

UHIs can also exacerbate the effects of heat waves, leading to an increased risk of heat stroke and other heat-related illnesses, particularly in vulnerable populations such as the elderly and those with pre-existing health conditions [4], [22], [23]. It has also been shown that urban heat islands can decrease

outdoor physical activity, as high temperatures can make it uncomfortable for people to spend time outside [24]. This can contribute to the overall decline in physical fitness and increase the risk of obesity and other health problems.

2.1.1 Urban heat dome

The rise in temperature within UHIs can result in the so-called urban heat dome flow, or urban heat island-induced circulation [25], [26]. This is caused by the temperature differences between urban and rural areas during calm weather with an inversion layer. The main contributing factors to this mean circulating flow are the horizontal pressure gradients between urban and rural areas and uneven plumes impacting the inversion layer. Urban heat domes are defined by converging inflow at the lower atmosphere levels, upward flow in the form of turbulent plumes over the urban area, diverging outflow at the upper atmosphere levels, and a dome-shaped boundary at the interface between the inversion layer and the diverging outflow region [27] as seen in Fig. 2.2.

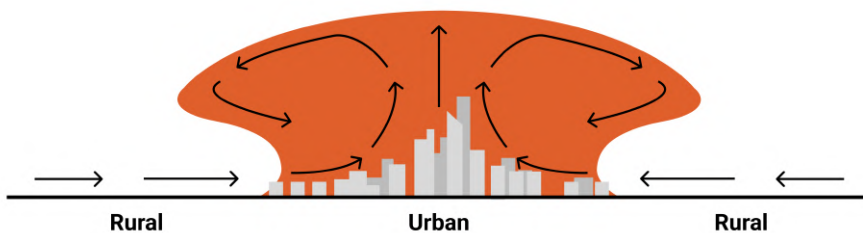


Figure 2.2: Urban heat dome, typical form of urban boundary layers caused by heat induced circulation. Adapted from [28]

The role of wind and atmospheric conditions in the spread of pollution and heat relief is significant. Without strong wind patterns, the air circulation in cities can be hindered, leading to an accumulation of pollution [29]. Additionally, this can inhibit cloud formation, leading to more sun exposure and increased heat in urban areas even further.

Overall, Urban Heat Islands and Urban heat dome flow are important and complex phenomena to consider in the context of climate change and urban development. It is important for cities to address the issue of UHIs in order to mitigate the negative impacts and create more livable and sustainable urban environments.

2.2 Man-made building materials

As mentioned in several above sections, heat absorbed and stored in building materials, such as concrete, asphalt and brick, will contribute to the heat island effect and, therefore, the urban microclimate. The reason is that these materials absorb and store heat during the day and then release it back into

the environment at night. This means that the cooling that usually happens when the sun has gone down is limited, leading to higher temperatures in the urban environment [19], [20].

Reflective surfaces can have both positive and negative effects on the microclimate. On one hand, they reflect incoming solar radiation back into the atmosphere, which can reduce the amount of heat absorbed by the urban environment, potentially leading to a cooler microclimate, especially during the summer months. On the other hand, if a large portion of the urban environment is covered in reflective surfaces, this reduced absorption of solar radiation can lead to lower air temperatures and increased air movement, which may be uncomfortable for pedestrians and discourage outdoor activity in the area. Additionally, reflected heat may produce higher mean radiant temperature at pedestrian level, which could affect the perceived temperature (further described in Section 2.5.2) of the environment [30].

Urban areas, which often have limited natural green spaces and are primarily covered in a variation of man-made materials, can therefore benefit from the use of materials that are less effective at retaining heat or the inclusion of features such as green roofs. These strategies can help to mitigate the heat island effect and offset the warming caused by heat-absorbing materials [31].

2.3 Vegetation and water bodies

Vegetation and water bodies can have a significant and positive impact on the urban microclimate by providing shade, evaporative cooling, increasing humidity, and reducing wind speed [32]. These effects can improve the overall comfort and well-being of urban residents and can also contribute to the attractiveness and livability of the urban environment. As such, urban planners and designers should consider the potential benefits of incorporating vegetation and water bodies into the urban environment when designing and managing the urban landscape.

Regarding UHIs and increased temperature in cities, vegetation and water bodies can help lower the urban environment's temperature, particularly during the summer months [32]–[34]. Vegetation, particularly trees, can provide shade and reduce the amount of solar radiation that is absorbed by the urban environment. Water bodies, such as ponds and lakes, can evaporate, which is the release of water vapor into the air by plants and cool the air around them through evaporative cooling. Vegetation can, through a process called evapotranspiration which releases vapour from the leaves of plants and moisture stored in the soil, also cool the environment to some extent as long as regular watering is maintained. This processes is sketched in Fig. 2.3.

Other factors that do not lower the temperature but increase comfort in other ways are humidity and wind. The humidity in the air can be increased by evaporation of water bodies and evapotranspiration vegetation. In addition to making the urban environment be perceived as more comfortable, the lower humidity can also help with better evaporative cooling of human bodies, and with less latent cooling load on buildings [35], [36]. Finally, vegetation can

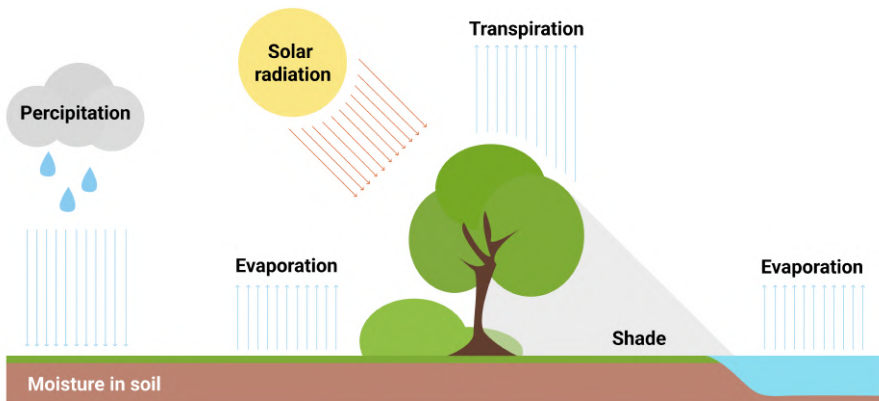


Figure 2.3: The process of cooling due to vegetation and water bodies.

provide windbreaks and reduce the wind speed in the urban environment. This could help to improve the wind comfort of a high wind speed area, however, it could also limit the ventilation and heat mitigation which could have the opposite effect. It is therefore important to evaluate if vegetation will provide positive or negative outcomes when it comes to urban comfort [37].

2.4 Urban furniture

Urban furniture, such as benches, bus shelters, solar shades, et cetera, can also have an impact on the microclimate of an urban area, though limited studies have been done on the specific impact. However, similarly to vegetation, urban furniture can affect factors like shade, wind, and heat absorption in the urban environment.

When urban furniture is placed in strategic locations, it can create pockets of shade that can help to reduce the temperature of the surrounding area. Urban furniture can also impact the wind speed and direction in an urban area. For example, a bus shelter can create a windbreak that can reduce wind speed and create a more sheltered microclimate. This can be especially important in cold climates, where wind can significantly lower the perceived temperature [38].

Finally, urban furniture can impact the microclimate by influencing the amount of heat absorbed by surfaces in the urban environment. For example, using urban furniture made of materials with a high albedo, or reflectivity, can help to reduce the amount of heat absorbed by the surrounding surfaces, as described further in Section 2.2.

2.5 Perceived urban comfort

Perceived urban comfort refers to an individual's subjective sense of well-being and comfort in an urban environment. This encompasses various qualitative and quantitative factors, including noise levels, air quality, thermal satisfaction, wind conditions, diversity of microclimatic environments, availability of green spaces, perception of safety and social interaction, accessibility to amenities, and aesthetics [39]–[41]. For example, the reputation of an area can affect urban comfort by influencing a person's perception of security, as an area with a negative reputation may be perceived as unsafe and uninviting. Furthermore, visually appealing urban environments can positively impact a person's overall well-being, regardless of microclimatic factors such as air quality or wind. While some factors are subjective and challenging to consider in city planning, others can be more easily evaluated.

Wind and heat are the two primary microclimatic factors affecting outdoor comfort. These comfort components can be quantified and modified relatively quickly and are significantly influenced by city planning. To evaluate the comfort level, standards referred to as comfort criteria are commonly utilized. These criteria take into account wind speed, direction, turbulence, temperature, and humidity, to determine the overall wind and thermal conditions in the area and their suitability for human activities.

2.5.1 Wind comfort criteria

Wind comfort criteria mainly consider the frequency of wind velocities and are often used by urban planners and designers to ensure that the wind conditions in a particular area are suitable for outdoor activities, such as walking or sitting in a park. There are several different wind comfort criteria that are used in different contexts and can vary depending on the location and the intended use of the area. Some standard wind comfort criteria include Davenport [42], multiple versions of the Lawson [43]–[45] and the Dutch wind nuisance standard [46].

Table 2.1: Lawson comfort criterion categories

Category	Velocity	Probability	Activity
1	> 1.8m/s	< 2%	Sitting long
2	> 3.6m/s	< 2%	Sitting short
3	> 5.3m/s	< 2%	Slow stroll
4	> 7.6m/s	< 2%	Walking fast
5	> 7.6m/s	$\geq 2\%$	Uncomfortable

One way to define a wind comfort criterium is by using a table like the one shown in Table 2.1 and Table 2.2. This first example, known as the Lawson wind comfort criterion, was introduced in 1975 [43] and categorizes wind comfort into five levels based on wind velocity probabilities. Each level is associated with a specific activity that is considered acceptable in the corresponding wind

condition. For instance, at low wind velocities, sitting for extended periods of time is acceptable, while at high wind speeds, discomfort is likely regardless of the activity being performed.

Table 2.2: Davenport comfort criterion categories

Category	Velocity	Probability	Activity
1	> 3.6m/s	< 1.5%	Sitting long
2	> 5.3m/s	< 1.5%	Sitting short
3	> 7.6m/s	< 1.5%	Walking leisurely
4	> 9.8m/s	< 1.5%	Walking fast
5	> 9.8m/s	\geq 1.5%	Uncomfortable
6	> 15.1m/s	\geq 0.01%	Dangerous

The Davenport and Lawson comfort criteria both use probability to determine appropriate wind velocities for different activities. However, the criteria differ in their specific velocity limits and probability thresholds. For example, under the Lawson criterion, the probability of wind speeds exceeding 3.6 m/s for short periods of sitting should be less than 2%, while Davenport defines the same activity as acceptable as long as the probability of speeds exceeding 5.3 m/s is less than 1.5%. In general, the two approaches have different standards for what is considered an acceptable wind velocity for different activities.

2.5.2 Heat comfort indices

For urban heat comfort, on the other hand, several factors can influence the comfort level, including temperature, humidity, wind speed, and the presence of heat-storing materials and reflective surfaces. This is because the physical temperature and the perceived temperature can vary quite a lot depending on the local air movement, humidity and radiation. In addition, the perceived comfort can also vary depending on the type of clothing worn, and the level of physical activity which means that the context of an area plays a difference in what a suitable temperature would be. Further, personal factors, such as age, gender, and the individual's tolerance for heat, will influence the experience with heat in a given context [47].

There are several heat comfort indices or criteria presented in the literature. These indices present numerical measures of urban heat comfort that consider some combination of the factors presented above, in contrast to the wind comfort criteria, which suggest a suitable activity. Examples of heat comfort indices used by urban planners are Wet-Bulb Globe Temperature (WBGT) [48], Universal Thermal Climate Index (UTCI) [49], and Physiological Equivalent Temperature (PET) [50]. The first two consider temperature, humidity, wind speed, and solar radiation to estimate the heat stress on the body, whereas the last also considers factors such as clothing insulation and physical activity.

Chapter 3

Numerical simulations of urban regions

3.1 Current practice

Urban Computational Fluid Dynamics simulations are a standard tool used in the planning and design of urban areas to predict and analyze the wind and thermal conditions in an urban environment. CFD can also be used to predict other factors of the urban environment, such as air pollution; however, this is not covered in this thesis.

3.1.1 Simulation application

Urban wind and heat simulations are numerical simulations used to model the flow of air, and potentially other fluids, in urban environments. These simulations are employed to understand how the flow of air around buildings, streets, and other urban features affects the movement of pollutants, the distribution of heat and moisture, and other factors that impact the comfort and well-being of urban residents. The results of these simulations can be used to evaluate the comfort level in an urban area, assess the potential impact of proposed development projects, and identify strategies to improve wind and thermal comfort of an urban environment.

Urban CFD simulations are typically performed using specialized software that is designed to simulate the flow of fluids around complex geometries. The simulations take into account a variety of factors, including the properties of the fluid, the shape and orientation of the urban features, and the boundary conditions, such as wind speed and direction.

These simulations can have a wide range of applications, including the design of energy-efficient buildings, the assessment of air quality in urban environments, and the prediction of wind loads on structures. They are also used to study the effects of weather patterns, such as heat waves, on urban environments and to develop strategies to mitigate the negative impacts of extreme weather

events. They are a powerful tool for understanding the complex interactions between the wind and urban environments and an important tool for urban planners, engineers, and other professionals working to create more livable and sustainable urban environments.

3.1.2 Set-up process

Setting up an urban CFD simulation involves several steps and can be a complex process, particularly if the simulation involves a large and detailed urban environment. Some of the key steps and issues involved in setting up an urban CFD simulation are described below.

The first step in setting up a simulation is defining the domain. This includes identifying the specific area of the city that will be studied and determining the necessary size of the surrounding area to avoid numerical errors. The level of detail in the simulation must also be determined, such as which buildings should be included and whether features like roads, trees, and other structures are relevant to the analysis.

The next step is to create a mesh of the simulation domain, which can be challenging due to the complex geometry of the built environment and, potentially, the local topography. The meshes used in CFD simulations need to be fine enough to capture the small-scale features of the flow, such as boundary layers and vortexes, but also need to be coarse enough to keep the size of the simulation tractable. This can be difficult to achieve in an urban environment because of the presence of many small-scale features, such as buildings and trees, that can affect the flow. Additionally, the presence of many obstacles can make it difficult to generate a mesh with good quality and smooth transitions. This all means that the process of meshing an urban domain can be time-consuming and require a high level of expertise.

Furthermore, the boundary conditions that define how the fluid interacts with the boundaries of the simulation domain have to be specified. In urban simulations, these may include the flow of traffic on roads, current wind conditions, and the exchange of heat and moisture between the indoor and outdoor environments. It can be difficult to accurately specify boundary conditions in an urban environment, particularly since it is hard to get accurate data on the actual conditions.

Once the simulation domain has been defined and meshed, and the boundary conditions have been specified, the CFD equations can be solved to simulate the fluid flow within the domain. Since the urban domains are large and detailed, this will likely be a computationally expensive process. It can also be challenging to validate and calibrate an urban CFD simulation, data available for comparison can be hard to come by and usually has a low resolution.

3.1.3 Numerical schemes and models

In addition to the above-presented steps of the set-up process, deciding what numerical schemes and models to use for solving the governing equations has

to be done. Many different types of numerical schemes and models that can be used in CFD, each with their own strengths and limitations.

In simulations of urban environments, the model used for turbulence is the most critical. Either the turbulence can be solved directly through Direct Numerical Simulations (DNS) or two main modelling approaches are typically used: Large Eddy Simulation (LES) and Reynolds-Averaged Navier-Stokes (RANS). These approaches differ in how they represent the small-scale turbulence in the flow.

Direct Numerical Simulations solves the Navier-Stokes equations, which describe the motion of fluids, on a very fine grid to resolve all flow scales. This way, a complete representation of the turbulence dynamics, including the smallest-scale turbulence structures, is achieved. DNS provides a detailed understanding of turbulence, however, it very computationally demanding and not feasible to capture Kolmogorov scale turbulence in an urban scale grid.

Large Eddy Simulation, on the other hand, uses a coarser grid and resolves the large-scale turbulence while modelling the turbulence at smaller scales using subgrid-scale models. The representation of turbulence dynamics becomes in a less accurate, but is computationally more efficient than DNS. This approach is sometimes used in current practice [12], [51], and could provide valuable insight about detailed flow dynamics.

Finally, RANS simulations involve averaging the governing equations over a large number of flow time scales, resulting in a set of equations that describe the mean flow field. This approach is relatively simple and computationally efficient, but it cannot capture the small-scale turbulence that occurs in the flow. RANS simulations are therefore suitable for predicting the mean flow field, such as the average wind speed and direction at a particular location in the urban environment, and commonly used [7], [9]–[12], [16]–[18], [37], [52].

The difference in computational requirements for Large Eddy Simulation (LES) and Reynolds-averaged Navier-Stokes (RANS) can be demonstrated by comparing the number of computational cells needed. Garcia et al. [51], [52] conducted urban scale simulations using both LES and RANS on an identical computational domain, with a slightly reduced size for the LES simulation to conserve computational resources. Despite the reduced domain size, the mesh size for the LES simulation was around 87 million cells, which is significantly larger than the 7.5 million cells used in the RANS simulation.

3.1.4 Best Practice Guidelines

To simplify the process of setting up the simulations appropriately and selecting numerical schemes and models, several Best Practice Guidelines (BPG's) have been developed. Mostly referenced are published by Franke et al. [9], Tominaga et al. [10], and Blocken [11] which all cover similar topics.

Firstly, the importance of using accurate and up-to-date data. If the geometries and other input data are not representative of the current situation, the results will not give meaningful output. This might seem obvious, but it can be hard to acquire appropriate data at this scale. It can also be helpful to have a clearly defined scope and objectives of the simulation to ensure that the

simulation is designed and run effectively.

As mentioned, the guidelines also give input regarding the appropriate models and methods. This also includes the necessary grid and domain size to achieve results with limited numerical errors. However, all the mentioned guidelines are based on the use of RANS and body-fitted meshes, which means that for other simulations all guidelines might not be appropriate.

The guidelines also cover validation of the simulated results to ensure that they are accurate and reliable. This can be done by comparing the results to real-world data or by conducting sensitivity analysis to test the robustness of the results.

3.1.5 Lacking in current practice

When reviewing CFD studies of the urban microclimate, well-explored and developed methods for wind simulations have been found [53]–[55], however for the heat, there is work to be done. One initial find is that heat modelling is not covered in any of mentioned BPG's suggesting that the knowledge on the subject is restricted. Regarding studies on heat modelling, there are several that consider solar radiation and diurnal variation of temperature in urban regions [17], [37], [56]–[59], but there are limited studies that considers the heat-absorbing capacity of different materials [17], [56].

Another important feature regarding temperature and heat in cities is cooling. Many studies have been done regarding the inclusion of cooling [37], [57], [60]–[62], but far from all heat simulations consider cooling due to vegetation and other natural features on the microclimate [17], [56]. It would be beneficial to plan studies that covers both heat-absorbing construction materials as well as cooling green and blue areas similar to Robitu et al. [37], to be able to analyzes their interaction further.

To the author's knowledge, the only study presented that has been able to replicate the dome shape effect of an urban heat island is by Fan et al. [59]. However, their study considers a quasi-steady state situation and not the periods surrounding sunrise and sunset when there are large variations in temperature. This also means that the heat-abortion is not solved, although radiation from walls is considered to an extent. Vegetation is not considered, although it is mentioned that the urban heat dome characteristics would be different in cities with abundant greenery.

Although air pollution is not covered in this thesis, there are related issues that are of importance when discussing what is lacking in the current practice. The main point is that there are limited computational studies where both heat and air pollution are covered simultaneously. The current practice of urban planning is typically based on different physical phenomena that are simulated in different simulation tools, which means that there is no coupling between the phenomena in addition to the fact that it requires more work for the designers to set-up different simulations.

3.2 IBOFlow

This work uses the flow solver IPS IBOFlow[®], developed by Fraunhofer-Chalmers Research Centre (FCC), to efficiently handle complex urban geometries and model fluid flow in urban regions. It is a numerical simulation software that utilizes the immersed boundary approach (see Section 3.2.1) to solve fluid dynamics. The solver employs steady-state Reynold’s averaged Navier-Stokes equations which are discretized and solved using the finite volume methodology on a Cartesian octree grid. The grid is automatically refined along the immersed boundaries of the ground and buildings, or at specific regions defined by the user, using an adapted grid refinement algorithm. The input geometries describing the local topography of the terrain and the buildings consist of oriented triangulated surface meshes automatically connected to the background grid.

The solver uses the segregated SIMPLEC (Semi-Implicit Method for Pressure Linked Equations Consistent) method [63], [64] to couple the pressure and velocity variables. This method first estimates the momentum equation using an initial pressure field, and then adjusts the pressure using the continuity equation. The variables are stored at the centers of the cells in a co-located grid configuration. To prevent pressure oscillations, the solver employs the Rhie-Chow [65] weighted flux interpolation method. The steady-state solver uses artificial time-stepping, and the equations are solved until all relative solution residuals are lower than a given threshold, or oscillatory convergence is reached [11]. The flow solver employs GPU-parallelisation to solve the linear equations to accelerate the simulations.

3.2.1 Immersed Boundary Method

The immersed boundary method is a numerical simulation technique, originally proposed by Peskin in 1982 [66], that is used to model fluid flow around a complex or deformable objects. One of the key features is that the immersed boundary method allows the governing equations to be solved in a simple Cartesian coordinate system, even when the simulated domain has complex geometries. This is useful because it allows a simulation to accurately represent complex geometries without the time-consuming processes of generating body-fitted meshes. In addition, the mesh quality will also not be affected by complex shapes.

For the immersed boundary method to work, the presence of the immersed solid or fluid boundaries has to be incorporated into the governing equations. Typically this is done by introducing a numerical source term that will replicate the effect of the boundary [67]. These governing equations, or the incompressible Navier-Stokes equations, are given as

$$\frac{\partial u_j}{\partial x_j} = 0, \quad (3.1)$$

$$\frac{\partial(\rho u_i)}{\partial t} + \rho u_j \frac{\partial u_i}{\partial x_j} = -\frac{\partial p}{\partial x_i} + \frac{\partial}{\partial x_j} \left(\mu \frac{\partial u_i}{\partial x_j} \right) + f_i, \quad (3.2)$$

where u is the velocity component in the subscript direction, x is the position, t is time, p is pressure, ρ is the fluid density, μ is the dynamic viscosity and f_i represents the numerical source term.

The immersed boundary can also be implemented through an implicit force. In this case, no source term is added to the governing equations; instead, a boundary condition is applied to the velocity at the boundary surface, which is immersed in the system [68]. This allows the simulation to accurately model the behavior of the system without introducing any additional sources or influences.

In this work the latter approach is taken, with the unique and second-order accurate method called *mirrored immersed boundary condition* introduced by Mark and van Wachem [68]. The method is briefly described in the following section.

3.2.1.1 Mirrored immersed boundary condition

The mirrored immersed boundary condition models the fluid flow along immersed boundaries using reflective symmetry over the immersed boundary. To be able to do this, interior cells and boundary cells has to be identified as illustrated in Fig. 3.1.

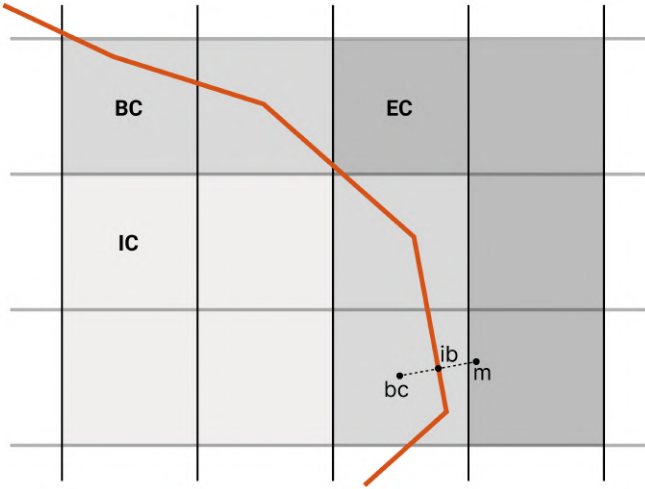


Figure 3.1: Distribution of interior cells (IC), boundary cells (BC) and exterior cells (EC) in the presence of an immersed boundary and representation of the mirroring of the boundary cell node (bc) over the immersed boundary (ib) to mirrored node (m). Adapted from [68]

The velocity in the boundary cells are set using an implicit Dirichlet boundary condition

$$u_i = u_i^{ib}, \quad (3.3)$$

where u_i^{ib} is the local velocity of the immersed boundary. In the mirroring immersed boundary method, the boundary cell node is reflected across the

immersed boundary to a point in the flow domain. The velocity of the boundary cell node is set so that it is equal to the velocity of the local segment of the immersed boundary as determined by a linear interpolation between the boundary cell node (bc) and the mirrored node (m) in the fluid domain as follows

$$u_i^{ib} = \frac{u_{bc} + u_m}{2}. \quad (3.4)$$

Note that this will result in a fictitious velocity field inside the immersed boundary. This velocity is excluded in the continuity equation to make sure that the mass flux over the immersed boundary is zero.

3.2.2 Turbulence modelling

As mentioned, IBOFlow is based on the RANS equations and include three different turbulence models that can be compared for the urban simulations; the Spalart-Allmaras, the realizable $k - \varepsilon$ and the $k - g$ SST model. The immersed boundary method can easily be employed for the RANS equations as (3.1) and (3.2) are solved using direct numerical simulation.

The Spalart-Allmaras turbulence model, originally developed for the aerospace industry, is a widely used RANS model for wall-bounded flows. It is a one-equation model, which solves for the turbulent kinetic energy, k , rather than a set of equations [69]. One of the main advantages of the Spalart-Allmaras model is that it is relatively simple to implement and computationally efficient. Additionally, it has been shown to produce good results for flows with complex geometries and high Reynolds numbers, which is suitable for the urban environment. However, it is important to note that the Spalart-Allmaras model has some limitations. One major drawback is its ability to predict free-shear flows, particularly in the case of turbulent jets. However, as the flow is often wall-bounded in the areas of interest in urban regions, this is not a main concern for these types of simulations.

The $k - \varepsilon$ model is the most common model used in computational fluid dynamics and is suggested for urban simulations in the BPG's [11]. It is a two-equation model meaning that an extra transport equation, the dissipation rate of turbulent kinetic energy, ε , is included to represent the turbulent properties of the flow [70]. While the k -epsilon model is a popular choice for many engineering simulations, it is known to underperform near walls and in flows with strong adverse pressure gradients. However, the realizable k -epsilon model [71] has been developed as an improvement of the standard k -epsilon model, it has been demonstrated to improve performance for boundary layers under strong adverse pressure gradients, rotating flows, separation, and recirculation, making it more suitable for urban flow simulations.

The $k - g$ SST model is an immersed boundary variant of the $k - \omega$ SST model that utilizes the Menter SST (shear-stress transport) [72], [73] blending function to improve the prediction of the turbulent viscosity near the wall. This blending function, which switches between the original Wilcox $k - \omega$ equation [74] close to walls and $k - \varepsilon$ in the free-stream, allows the model to adapt to flows with complex geometry, such as in urban environments. To adapt to the

immersed boundary setting, the specific rate of dissipation, ω , typically used in the model, is changed to the turbulence time scale $g^2 = 1/C_\mu\omega$ [75] making it the $k - g$ model. This hybrid method provides more accuracy but is less computationally efficient than both previously mentioned models.

3.2.3 Heat transfer modelling

To be able to predict the temperature distribution and heat transfer in urban region flows, the heat has to be modelled. These models are used to simulate the heat transfer between a fluid and a solid surface, as well as the heat transfer within the fluid and solids themselves. This section will cover the various heat transfer models that are implemented in IBOFlow. At this stage of the development, the code handles convection, conduction and diffusion. Another important heat transfer phenomenon in urban heat simulations is radiation, both solar radiation and from building materials, which is planned for future development.

Typically in CFD, the temperature of the flowing fluid is what is being solved, which means that the heat transfer through the fluid is the main mechanism involved. In urban simulations, the temperature of the air is highly tied to the surface temperatures of building materials, however, the surface temperatures are also dependent on the air temperature. Therefore it can be of importance to solve also the temperature in the solid structures and couple both these heat transfer phenomena.

3.2.3.1 Heat transfer in fluids

To compute the heat transferred in fluids, the temperature field is calculated using a transport equation for temperature, where the fluid temperature at the solid-fluid interface is set to the solid temperature using an immersed boundary methodology [76].

The transfer of heat through convection can be categorized into two types: forced convection, driven by fluid motions such as wind, and natural convection, resulting from buoyancy-driven flow. To model the convective transport, an effective conductivity is included in the temperature equation. When utilizing turbulence modeling, the effective conductivity is represented as a turbulent conductivity instead of the actual conductivity of the fluid. Natural convection, caused by temperature-induced density variations in the fluid, is modeled in the momentum equation using the Boussinesq approximation. This approximation considers the fluid density difference to be a product of temperature, gravity, and the thermal expansion coefficient.

3.2.3.2 Coupled fluid and solid heat transfer

Coupling between fluid and solid heat transfer is achieved through the use of a conjugate heat transfer model. This model first defines the proportion of fluid and solid in each cell and face, allowing for the active solid cells to be determined and included in the discretized heat equation [77].

A fluid and solid model is then used to simulate the temperature transport, and temperature diffusion inside and between different solids. In this part, heat transfer is modeled separately for the solid and fluid phases, and the two phases are coupled through the use of physical boundary conditions at the interface. The fluid temperature is set to the local solid temperature by a Dirichlet immersed boundary condition. The solid is coupled to the fluid by a Neumann heat flux immersed boundary condition. The heat flux is proportional to the fluid conductivity, the local fluid temperature gradient and surface. When the boundary layer is not resolved the solid temperature and fluid gradients are estimated from wall functions.

Typically the heat boundary layer in cities are very thin and hard to resolve. In these cases the heat flux can be estimated by a Heat Transfer Coefficient (HTC). With this approach the flux is estimated as the temperature difference between the local solid temperature and a fluid reference temperature times the HTC and the local area. The heat flux is then applied in the same way as the resolved one with a Neumann immersed boundary condition [78].

3.2.4 Wall functions

For high Reynolds number flows, where the first grid point lies outside the viscous sub-layer, wall functions are used to estimate the stresses on the ground and the buildings. The flow solver identifies the cells inside the fluid but close to the surface and for each such cell, wall functions are used to calculate the local fluid stress on the wall. The stress is then applied to the local wall by an explicit force. The momentum and the different turbulence models have different modifications or wall shifts [79]–[81].

In urban simulations, the common practice, as mentioned in the best practice guidelines [9]–[11], is to explicitly model buildings at the center of the domain surrounding the area of interest. Further away from the center, closer to the boundaries, the buildings are implicitly modelled through surface roughness parameters. These roughness parameters are employed as a wall function. Typically the implicit modelling of roughness in atmospheric boundary layers is expressed by the introduction of an aerodynamic roughness length z_0 [82], [83]. This parameter is usually not available in most numerical tools, including IBOFlow, instead, the roughness is modelled as wall functions expressed in terms of a sand grain roughness height k_s [84]. A typical conversion between the the Davenport-Wieringa roughness length, z_0 , and the sand grain height, k_s for atmospheric boundary layers is defined as $k_s = 30z_0$ [84].

Chapter 4

Selected Results

This chapter covers some selected results from the appended papers as well as the preliminary results from introducing heat into the wind tunnel validation case.

4.1 Wind tunnel validation

In both Paper A and Paper B, the flow solver is validated using the Particle Image Velocimetry (PIV) experimental data by Allegrini [85]. The experiment is run over a compilation of variously sized blocks in a wind tunnel to describe an idealized urban area of a 5x5 row configuration of buildings with straight, continuous streets forming canyons. In a central street canyon, the air velocity is measured using PIV. Some modifications are made to this setup to create five different cases to study the flow field, namely cases A-E. Case A is the case just described, while the other cases consist in changing the inclination of the roof of the leading building (cases B and C) or changing the width of the leading and trailing (cases D and E) building in the measured canyon.

Paper A covers the validation of Case C, which has a pitch roof building on the leading edge of the canyon which will be briefly presented in this section. Further validation of case A can be found in Paper B. The inlet velocity is 1.94 m/s and the wind tunnel data correspond to a vertical and horizontal velocity plane from Particle Image Velocimetry measurements, shown in Fig.4.1 where an additional row of buildings has been added after testing of an appropriate simulation domain.

The simulation grid consists of base cell size of $0.05 \times 0.05 \times 0.05$ m. The grid is refined around the parts of the ground and buildings that are closest to the walls. The ground and buildings on the sides of the domain are refined twice, whereas the six buildings in the middle column, where the PIV-planes are situated, are refined even further, up to a total of four refinements, resulting in an approximate total of five million cells in the entire domain. A grid optimization study has been performed to accurately evaluate the minimum number of cells to solve the mean flow field inside the canyon. The three grids

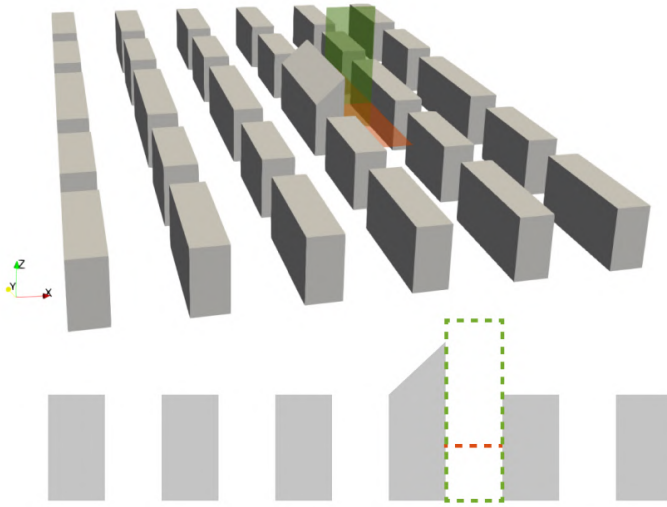


Figure 4.1: Top: 3D visualization of the domain where the red and green planes show the horizontal and vertical PIV-planes, respectively. Bottom: 2D side view, PIV-planes showed as dashed lines in green and red.

employ two, three and four refinements in the cells surrounding the measured canyon. The results are presented in Fig. 4.2 and Fig. 4.3.

In Fig. 4.2 the contours of the in-plane mean velocity magnitude on the vertical plane for the experimental (a) and the numerical data (b-d) at different

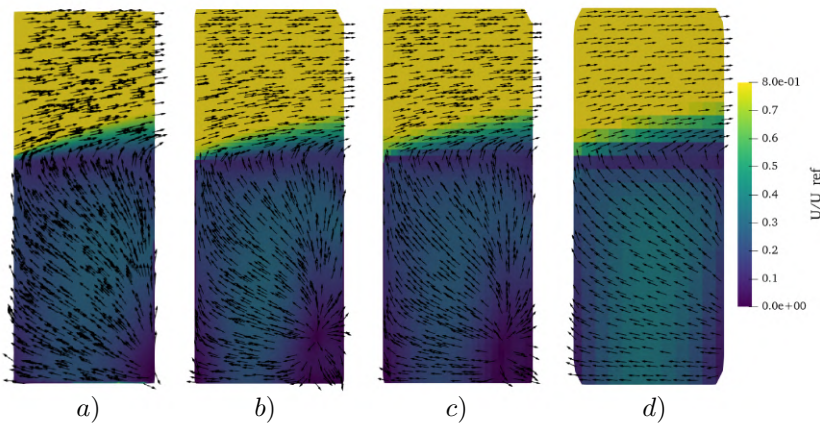


Figure 4.2: Contour plots and streamlines of the in-plane mean velocity magnitude on the vertical plane. The panels represent the PIV data (a) followed by the results of three simulations with different grid resolutions, b) 4 refinements, c) 3 refinements, and d) 2 refinements

resolutions are shown. There is fair agreement between the experimental data for the four and three refinements where the recirculation region in the lower right corner of the canyon is captured. The simulation in the most coarse grid shows a large part of the canyon with low-velocity magnitude probably induced by numerical dissipation. This could indicate that some important fluid dynamics phenomena might be missed if the mesh is not refined well enough.

A more quantitative comparison between the different solution fields, is shown in Fig. 4.3 for the vertical and horizontal profile of the horizontal mean velocity component. The profiles confirm the qualitative impression. The coarser grid predicts a lower mean velocity inside the canyon close to the ground to then become similar after the roof level. To conclude, the grid study shows that 24 cells per canyon are sufficient. A coarser mesh can give fair results overall, but fails to predict detailed results of the flow field inside the canyon.

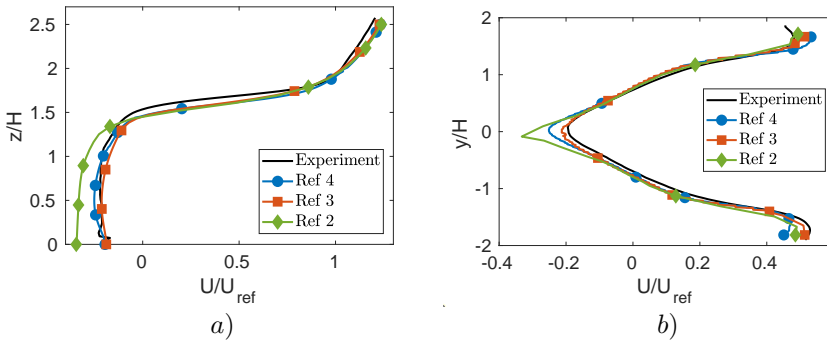


Figure 4.3: a) Vertical and b) horizontal profiles of the horizontal average velocity component at the center of the street canyon for Case C. The simulation results with grid refinements (solid lines with symbols) are compared against PIV experimental data (solid black line).

4.2 Urban scale simulations

In Paper B, the flow solver is applied at urban scale. The wind pattern and wind comfort is simulated in an urban area of Gothenburg, Sweden. The study area is a complex terrain of $2600 \times 2600 \times 500 \text{ m}^3$ and features buildings modeled explicitly in the center and implicitly, as described in Section 3.2.4, along the boundaries. The computational grid consists of around 10 million cells with a base cell size of $20 \times 20 \times 20 \text{ m}^3$ that is refined up to four times in the area of interest. A simulation of one wind direction takes approximately five hours on the HPC2N supercomputer Kebnekaise running on 10 CPU cores and a NVIDIA V100 (Volta) GPU, the mesh generation phase is negligible.

Firstly, the wind pattern simulations using IBOFlow are compared to a commercial software, MISKAM, typically used in urban planning. MISKAM

assumes a flat ground everywhere, but can add larger terrain variations, like the hill on the north-eastern side of the computational domain in this case. IBOFlow is capable of accounting for altitude differences. In Figure 4.4 a comparison of a) MISKAM and b) IBOFlow can be seen at 1.5 m height above the local terrain level. The shown result is the annual average wind in the area, calculated from measured probabilities of wind conditions. The calculations are made by considering wind simulations of 36 directions for one wind speed that is re-scaled to six different wind speeds to generate all measured wind conditions. Further explanations of how the annual average wind is calculated can be found in Paper B.

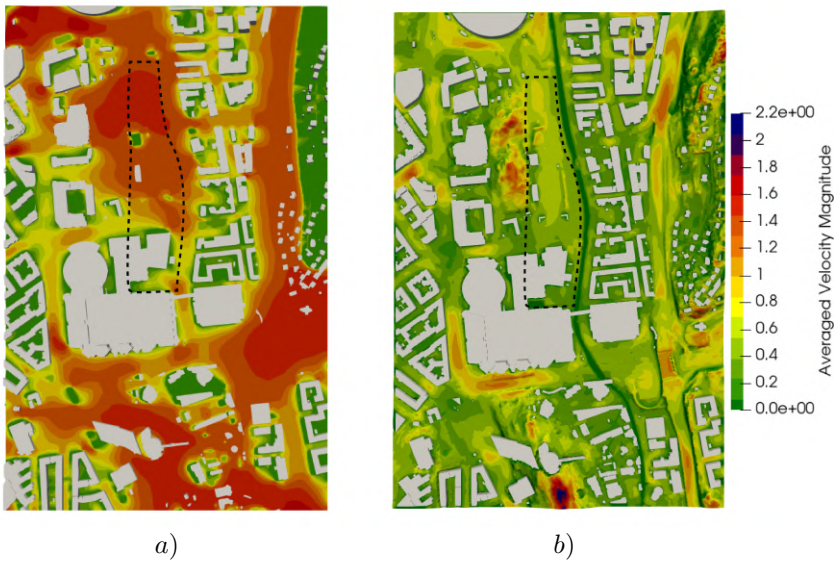


Figure 4.4: a) Velocity in the cell 0.9 - 2 m above the flat ground for reference case in MISKAM, b) Velocity over a plane 1.5 m above ground level for simulation using IBOFlow. Black dashed lines mark a flat region of the domain.

Comparing the two planes at pedestrian level in Fig. 4.4, the velocity fields are relatively different. Mainly, the simulations made in MISKAM generate larger velocity magnitudes than IBOFlow. There is a flat area, marked in dashed black lines in Fig. 4.4, where a qualitative comparison can be made. Although the wind speeds differ, it is in this flat region where we have the best correspondence between the two models. Qualitatively the same flow structures in comparison to the surrounding regions can be seen. However, given the different results using two different terrains, we recommend to solve the local terrain topography for wind comfort simulations in an urban area.

4.2.1 Wind comfort

The wind in urban regions has also been evaluated by using the wind comfort criteria as explained in Section 2.5.1. Fig. 4.5 show a comparison of the Lawson and Davenport wind comfort criteria over the computational domain at pedestrian height. According to the Lawson model, all regions are suitable for short periods of sitting, with the exception of a small area on a hill along the bottom boundary. However, this same region is appropriate for slow strolling and not classes as uncomfortable. The Davenport criteria also indicate that the majority of regions are suitable for sitting, but there are some additional areas that fall into comfort level three, where leisurely walking is recommended. This suggests that while wind comfort is not an issue in these regions, however, there may be concerns with heat and air pollution ventilation due to low velocities

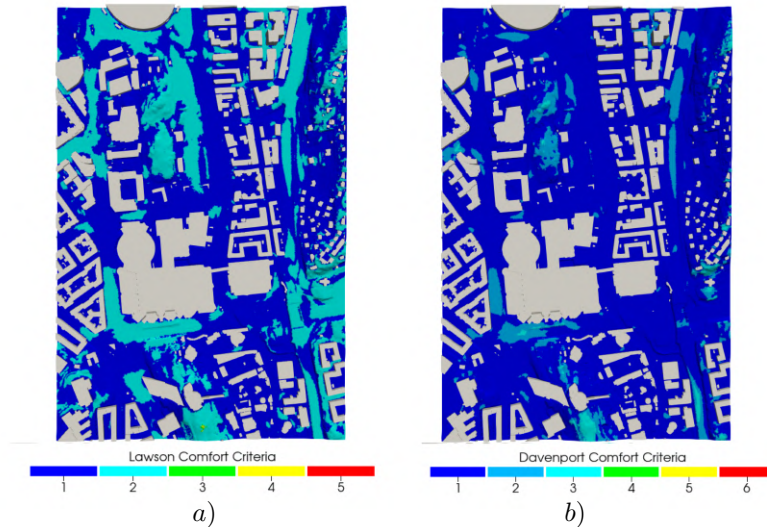


Figure 4.5: a) Lawson comfort criteria based on hourly data over one year. b) Davenport comfort criteria based on hourly data over one year. Both shown at pedestrian height.

4.3 Heat simulations

The experiment used for the isothermal validation in Section 4.1 has also been performed for cases with a heated ground plate [85]. The different building configurations are the same with the addition of a heated ground plate under the street canyon with the PIV-planes and the closest surrounding buildings. These experiments will be used to validate the implementation of heat models in IBOFlow, so that the numerical framework can be used to simulate the important heat phenomena of the urban microclimate. In this Section, the initial part of this validation process is shown, which means that the heat

models are still being developed to capture the difference in physics seen in these results.

The initial results shown in Fig. 4.6 are for the same Case C as in Section 4.1 but with a lower inlet velocity of 0.367 m/s as to limit the strength of convection, and thereby cover more physical phenomena, and an inlet temperature of 23 °C and ground plate temperature of 60 °C. In these results, the temperature of the walls have been kept constant at 23 °C as the buildings in the experiments are covered in cork to insulate them from the heated plate. In the comparison of the a) experimental and b) simulated results in Fig. 4.6, it was found that the cork most likely does not insulate as well as expected, and that the building walls are probably heated by the ground plate. Therefore, further testing was made by introducing slightly heated walls, setting the wall temperature to half of the heated plate ie. 30 °C, to see if the simulated results would match the experimental ones better, which can be seen in Fig. 4.6c. The temperature does match better in this case, seeing that the heat does rise along the trailing edge building wall, however, there are still issues to resolve.

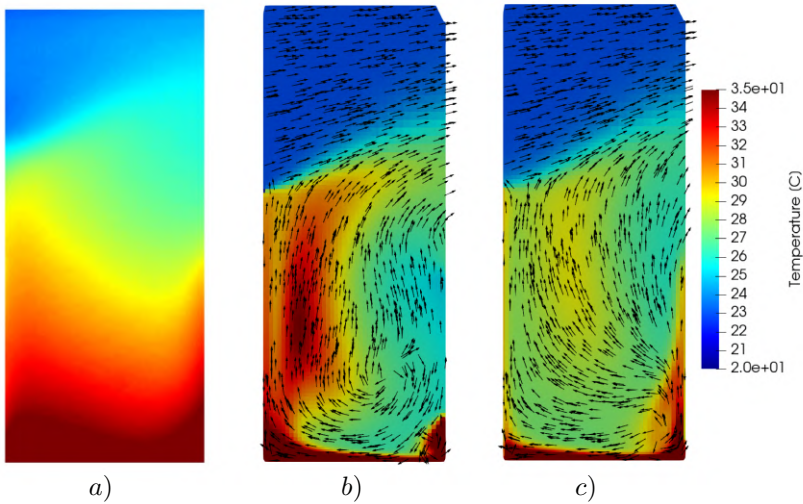


Figure 4.6: Temperature distribution of Case C with an inlet air temperature of 23 °C and heated ground plate of 60 °C from a) the experiment, b) simulation with lateral walls kept at 23 °C c) simulation with lateral wall temperature set to 30 °C. The simulated results also include the velocity streamlines.

For example, the convection is very strong and the temperature stratification caused by diffusion and buoyancy from the heated plate is barely present. One possible reason for this phenomenon is that the air temperature diffusion is much slower than the convection of heat. This means that the convection effect will be dominant in the final results, and the natural stratification from for example ground diffusion is barely present. To address both the issue with the heated walls and the difference in timescale of the diffusion and convection, an adaptive conjugated heat transfer model has been introduced in IBOFlow.

In this adaptive timescaling method the conjugated heat transfer is first simulated to steady state, then only the conjugated fluid and solid heat with diffusion based artificial time steps is solved excluding the convection. Finally, the conjugated heat transfer is solved to steady state to include updated buoyancy effects.

Alongside this adaptive model, the pure conjugated heat transfer case without the coupling with the heat transfer coefficient can be used, and some initial results can be seen in Fig. 4.7. What can be seen in this figure but not in others is both the diffusive and convective nature of the heat transfer, although the solution does not converge towards the steady state so the diffusion is not as present in all iteration steps. Both these models are currently being tested and tuned to achieve a fair balance between the heat transfer phenomena.

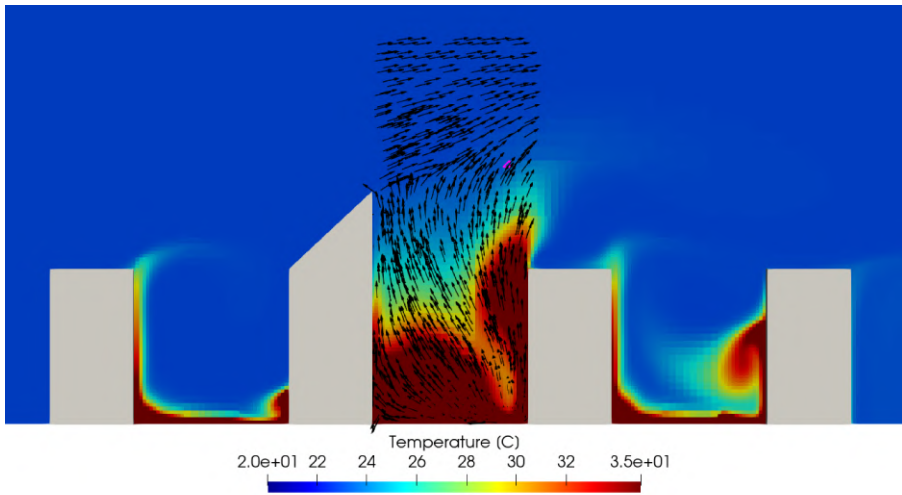


Figure 4.7: Temperature distribution of Case C with heated ground plate using conjugated heat transfer

Another possible issue could be that the Boussinesq approximation does not hold for these large temperature gradients, which are much larger than what is expected to be in an urban setting. This would mean that this modelling approach would not be able to recreate this specific case and that another validation case, with temperatures closer to those in an urban area, would have to be used. On the other hand, the velocity field does show that buoyancy is present and it takes on the same directional shape and magnitude as the experimental results, as shown in Fig. 4.8.

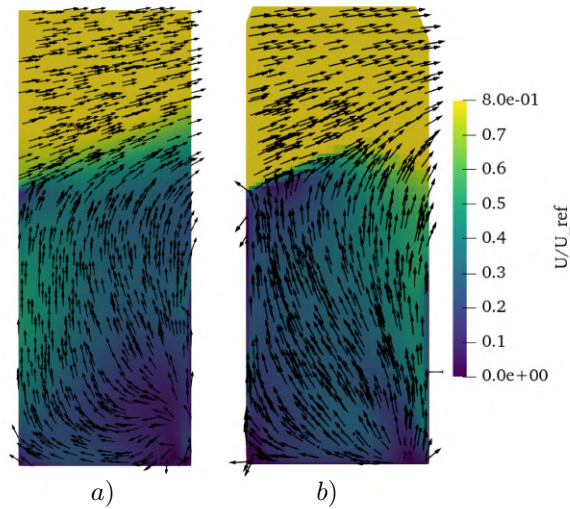


Figure 4.8: Velocity distribution of Case C with heated ground plate for a) the experiments and b) the conjugated heat transfer

Overall, these initial results of the heat simulation show potential of simulating heat in urban regions, however there is work to be done before we have a validated model.

Chapter 5

Summary of papers

5.1 Paper A

P. Vanky, A. Mark, F. Hunger, M. Haeger-Eugensson, J. Tarraso, M. Adelfio, A. Sasic Kalagasidis, G. Sardina, Addressing wind comfort in an urban area using an immersed boundary framework. *Technische Mechanik-European Journal of Engineering Mechanics*, accepted, in press

Division of work

In addition to the role as main author of this paper, all simulations, graphs and illustration has been made by Vanky. Mark and Hunger has provided the code and support regarding it as well as written the original draft of the flow solver sections. Haeger-Eugensson, Tarraso and Adelfio has provided valuable insight and discussions regarding urban planing and designing. Haeger-Eugensson and Sasic Kalagasidis have acquired validation and measurement data from different sources. Sardina has provided valuable feedback on all parts of the work and has supervised the work together with co-supervisors Mark and Sasic Kalagasidis. All co-authors have been responsible for reviewing the manuscript.

Summary and discussion

The purpose of this paper is to validate an immersed boundary framework developed by Fraunhofer Chalmers Research Centre (FCC) using wind tunnel data of an idealized city block. The framework aims to ease the pre-processing of urban simulations by eliminating the complex process of meshing complex geometries. The results show good agreement with the experimental data and guidelines has been provided on the choice of minimum grid sizes required to capture the relevant flow structures inside a canyon accurately. In addition to the validation the numerical framework has been applied to estimate the wind comfort of the idealized urban area using wind conditions measured over one year in Gothenburg, Sweden.

5.2 Paper B

P. Vanky, A. Mark, F. Hunger, M. Haeger-Eugensson, J. Tarraso, M. Adelfio, A. Sasic Kalagasidis, G. Sardina, Evaluation of Wind in Urban Regions with Complex Local Topography Using an Immersed Boundary Framework. *Submitted for journal publication*, under review

Division of work

In addition to the role as main author of this paper, all simulations using IBOFlow, graphs and illustration has been made by Vanky. Mark and Hunger has provided the code and support regarding it. Haeger-Eugensson, Tarraso and Adelfio has provided valuable insight and discussions regarding urban planing and designing. Haeger-Eugensson and Sasic Kalagasidis have acquired validation and measurement data from different sources. Sardina has provided valuable feedback on all parts of the work and supervised the work together with co-supervisors Mark and Sasic Kalagasidis. All co-authors have been responsible for reviewing the manuscript.

Summary and discussion

The paper covers the validation of an immersed boundary framework developed by Fraunhofer Chalmers Research Centre (FCC) against wind tunnel data of an idealized city block. Additionally, the framework is used to calculate the annual average wind over a real urban area and the results are compared to those obtained using another standard CFD code. This comparison highlights the importance of accurately representing complex terrain topographies in order to capture all flow phenomena. Finally, wind comfort criteria are calculated in the same region and guidelines on grid size, turbulence model, computational domain, and wind direction are provided.

Chapter 6

Concluding remarks

6.1 Summary

To summarize, sustainable urban development is becoming increasingly important, and evaluation of the urban microclimate is essential. Numerical simulations are particularly useful as they can predict microclimate conditions with large flexibility in domain changes. However, they are often not utilized in the urban planning process until the final stages of a project, due to the complexity of these tools, at which point it is often too late to make significant design changes. This thesis, therefore, covers a literature review of the current issues with the current practice and the development of a more accessible and user-friendly numerical framework for urban planners.

The literature review conducted on current methods of urban simulations revealed that while there are well-developed methods for simulating wind in the urban microclimate, there is still work to be done in the area of heat simulation. Not only are the available BPG's lacking in covering heat modelling, but studies on the subject are also limited. Studies have been found on solar radiation and temperature variation, however, studies on the heat-absorbing capacity of building materials and cooling effects from vegetation and natural features are restricted. Additionally, there is a need for studies that replicate the urban heat island effect in general, but especially during periods of large temperature variation such as sunrise and sunset. Another barrier identified in the current urban planning practice is the use of separate tools to simulate different physical phenomena. This leads to difficulties in understanding the interplay between them while at the same time requiring increased effort from designers.

In this thesis, the potential of the numerical immersed boundary framework IBOFlow[®] as a tool that can be put in the hands of urban planners to evaluate the urban microclimate at the early stages of the design processes has been presented. The new framework eliminates the complex pre-processing of urban regions by the use of automatically generated Cartesian octree grid meshes where the complex geometries are represented directly by the immersed boundary methodology instead of body-fitted meshed. The wind simulations in the framework have been validated against wind tunnel experiments, showing

good agreement and ensuring that the simulation results provide an accurate representation of wind conditions. Additionally, it was found that incorporating complex local terrain is essential for generating realistic results and thereby accurately predict the wind conditions in urban designs. The framework also shows potential as a comprehensive tool for simulating urban microclimate including more relevant physics, as shown in the initial results including heat modelling.

6.2 Future work

The future direction of this project centers on incorporating heat dynamics into urban simulations. Not only in terms of convection and diffusion from heated surfaces as briefly described in this thesis, but also other heat phenomena. The next steps include introduction of solar radiation as a heating source. Efforts are also being made to develop and include simplified models for heat storage in building materials to reduce computational costs. With the inclusion of solar radiation and heat storage, the transient nature of heat evolution in cities has to be address further as the current framework is a steady-state solver.

Additionally, the inclusion of models for the cooling effect of evaporation and evapotranspiration from vegetation and water bodies is crucial for simulating realistic temperatures. The next steps also include exploring the modeling of vegetation as wind breaks and how to include the vegetation in the computational domain.

Furthermore, the goal is to develop a comprehensive tool for evaluating the urban microclimate that includes all necessary physics. A future task would, therefore, also be to evaluate more thoroughly, what physics are necessary include in addition to wind and heat. It has already been mentioned that pollution is not covered in this thesis, but it would be a future goal to start incorporating those phenomena as well.

Bibliography

- [1] United Nations, Department of Economic and Social Affairs, Population Division. “World Urbanization Prospects: The 2018 Revision.” Online Edition. (2018) (cit. on p. 3).
- [2] D. o. E. United Nations and S. A. S. Development, *Transforming our world: The 2030 agenda for sustainable development*, General Assembly, 2015. [Online]. Available: <https://sdgs.un.org/2030agenda> (cit. on p. 3).
- [3] B. Blocken and J. Carmeliet, “Pedestrian wind environment around buildings: Literature review and practical examples,” *Journal of Thermal Envelope and Building Science*, vol. 28, no. 2, pp. 107–159, 2004. DOI: <https://doi.org/10.1177/1097196304044396> (cit. on pp. 3, 4).
- [4] H. Huang, X. Deng, H. Yang, S. Li *et al.*, “Spatial evolution of the effects of urban heat island on residents’ health,” *Tehnički vjesnik*, vol. 27, no. 5, pp. 1427–1435, 2020. DOI: <https://doi.org/10.17559/TV-20200503211912> (cit. on pp. 3, 4, 8).
- [5] R. Ewing and F. Rong, “The impact of urban form on us residential energy use,” *Housing Policy Debate*, vol. 19, no. 1, pp. 1–30, 2008. DOI: <https://doi.org/10.1080/10511482.2008.9521624> (cit. on pp. 3, 4, 8).
- [6] J. E. Cermak *et al.*, “Wind tunnel studies of buildings and structures,” American Society of Civil Engineers, 1999 (cit. on p. 3).
- [7] S. Reiter, “Assessing wind comfort in urban planning,” *Environment and Planning B: Planning and Design*, vol. 37, no. 5, pp. 857–873, 2010 (cit. on pp. 3, 17).
- [8] E. Krüger, F. Minella and F. Rasia, “Impact of urban geometry on outdoor thermal comfort and air quality from field measurements in Curitiba, Brazil,” *Building and Environment*, vol. 46, no. 3, pp. 621–634, 2011 (cit. on p. 3).
- [9] J. Franke, A. Hellsten, K. Schlünzen and B. Carissimo, “Best practice guideline for the CFD simulation of flows in the urban environment—a summary,” in *11th Conference on Harmonisation within Atmospheric Dispersion Modelling for Regulatory Purposes, Cambridge, UK, July 2007*, Cambridge Environmental Research Consultants, 2007 (cit. on pp. 4, 17, 23).

- [10] Y. Tominaga, A. Mochida, R. Yoshie *et al.*, “AIJ guidelines for practical applications of CFD to pedestrian wind environment around buildings,” *Journal of Wind Engineering and Industrial Aerodynamics*, vol. 96, no. 10–11, pp. 1749–1761, 2008. DOI: <https://doi.org/10.1016/j.jweia.2008.02.058> (cit. on pp. 4, 17, 23).
- [11] B. Blocken, “Computational fluid dynamics for urban physics: Importance, scales, possibilities, limitations and ten tips and tricks towards accurate and reliable simulations,” *Building and Environment*, vol. 91, pp. 219–245, 2015. DOI: <https://doi.org/10.1016/j.buildenv.2015.02.015> (cit. on pp. 4, 17, 19, 21, 23).
- [12] Y. Toparlar, B. Blocken, B. Maiheu and G. Van Heijst, “A review on the CFD analysis of urban microclimate,” *Renewable and Sustainable Energy Reviews*, vol. 80, pp. 1613–1640, 2017 (cit. on pp. 7, 17).
- [13] L. Howard, *The Climate of London: Deduced from Meteorological Observations Made at Different Places in the Neighbourhood of the Metropolis. In Two Volumes. Vol. II.* W. Phillips, 1820, vol. 2 (cit. on p. 7).
- [14] G. Manley, “On the frequency of snowfall in metropolitan England,” *Quarterly Journal of the Royal Meteorological Society*, vol. 84, no. 359, pp. 70–72, 1958 (cit. on p. 7).
- [15] Z. Yu, G. Yang, S. Zuo, G. Jørgensen, M. Koga and H. Vejre, “Critical review on the cooling effect of urban blue-green space: A threshold-size perspective,” *Urban Forestry & Urban Greening*, vol. 49, p. 126 630, 2020 (cit. on p. 7).
- [16] J. Allegrini, V. Dorer and J. Carmeliet, “Influence of the urban microclimate in street canyons on the energy demand for space cooling and heating of buildings,” *Energy and Buildings*, vol. 55, pp. 823–832, 2012 (cit. on pp. 7, 17).
- [17] N. Antoniou, H. Montazeri, M. Neophytou and B. Blocken, “CFD simulation of urban microclimate: Validation using high-resolution field measurements,” *Science of the total environment*, vol. 695, p. 133 743, 2019. DOI: <https://doi.org/10.1016/j.scitotenv.2019.133743> (cit. on pp. 7, 17, 18).
- [18] A. Kubilay, D. Derome and J. Carmeliet, “Coupling of physical phenomena in urban microclimate: A model integrating air flow, wind-driven rain, radiation and transport in building materials,” *Urban climate*, vol. 24, pp. 398–418, 2018 (cit. on pp. 7, 17).
- [19] T. Oke, G. Johnson, D. Steyn and I. Watson, “Simulation of surface urban heat islands under ‘ideal’ conditions at night part 2: Diagnosis of causation,” *Boundary-Layer Meteorology*, vol. 56, no. 4, pp. 339–358, 1991 (cit. on pp. 8, 10).
- [20] Y.-H. Kim and J.-J. Baik, “Maximum urban heat island intensity in Seoul,” *Journal of Applied Meteorology*, vol. 41, no. 6, pp. 651–659, 2002 (cit. on pp. 8, 10).

- [21] C. A. Bradley and S. Altizer, "Urbanization and the ecology of wildlife diseases," *Trends in ecology & evolution*, vol. 22, no. 2, pp. 95–102, 2007 (cit. on p. 8).
- [22] A. Smargiassi, M. S. Goldberg, C. Plante, M. Fournier, Y. Baudouin and T. Kosatsky, "Variation of daily warm season mortality as a function of micro-urban heat islands," *Journal of Epidemiology & Community Health*, vol. 63, no. 8, pp. 659–664, 2009. DOI: <http://doi.org/10.1136/jech.2008.078147> (cit. on p. 8).
- [23] Y. Rydin, A. Bleahu, M. Davies *et al.*, "Shaping cities for health: Complexity and the planning of urban environments in the 21st century," *The lancet*, vol. 379, no. 9831, pp. 2079–2108, 2012. DOI: [https://doi.org/10.1016/S0140-6736\(12\)60435-8](https://doi.org/10.1016/S0140-6736(12)60435-8) (cit. on p. 8).
- [24] J. K. Vanos, "Children's health and vulnerability in outdoor microclimates: A comprehensive review," *Environment international*, vol. 76, pp. 1–15, 2015 (cit. on p. 9).
- [25] B. Findlay and M. Hirt, "An urban-induced meso-circulation," *Atmospheric Environment (1967)*, vol. 3, no. 5, pp. 537–542, 1969. DOI: [https://doi.org/10.1016/0004-6981\(69\)90043-2](https://doi.org/10.1016/0004-6981(69)90043-2) (cit. on p. 9).
- [26] N. Zhang, X. Wang and Z. Peng, "Large-eddy simulation of mesoscale circulations forced by inhomogeneous urban heat island," *Boundary-layer Meteorology*, vol. 151, no. 1, pp. 179–194, 2014. DOI: <https://doi.org/10.1007/s10546-013-9879-x> (cit. on p. 9).
- [27] Y. Fan, J. C. R. Hunt and Y. Li, "Buoyancy and turbulence-driven atmospheric circulation over urban areas," *Journal of Environmental Sciences*, vol. 59, pp. 63–71, 2017. DOI: <https://doi.org/10.1016/j.jes.2017.01.009> (cit. on p. 9).
- [28] T. R. Oke, G. Mills, A. Christen and J. A. Voogt, *Urban climates*. Cambridge University Press, 2017 (cit. on p. 9).
- [29] Y. Abbassi, H. Ahmadikia and E. Baniasadi, "Prediction of pollution dispersion under urban heat island circulation for different atmospheric stratification," *Building and Environment*, vol. 168, p. 106374, 2020. DOI: <https://doi.org/10.1016/j.buildenv.2019.106374> (cit. on p. 9).
- [30] A. Salvati, M. Kolokotroni, A. Kotopouleas, R. Watkins, R. Giridharan and M. Nikolopoulou, "Impact of reflective materials on urban canyon albedo, outdoor and indoor microclimates," *Building and Environment*, vol. 207, p. 108459, 2022 (cit. on p. 10).
- [31] P. E. Phelan, K. Kaloush, M. Miner *et al.*, "Urban heat island: Mechanisms, implications, and possible remedies," *Annual Review of Environment and Resources*, vol. 40, pp. 285–307, 2015 (cit. on p. 10).
- [32] K. R. Gunawardena, M. J. Wells and T. Kershaw, "Utilising green and bluespace to mitigate urban heat island intensity," *Science of the Total Environment*, vol. 584, pp. 1040–1055, 2017 (cit. on p. 10).

- [33] D. H. Duarte, P. Shinzato, C. dos Santos Gusson and C. A. Alves, "The impact of vegetation on urban microclimate to counterbalance built density in a subtropical changing climate," *Urban Climate*, vol. 14, pp. 224–239, 2015 (cit. on p. 10).
- [34] P. Ampatzidis and T. Kershaw, "A review of the impact of blue space on the urban microclimate," *Science of The Total Environment*, vol. 730, p. 139068, 2020 (cit. on p. 10).
- [35] P. E. Thornton and S. W. Running, "An improved algorithm for estimating incident daily solar radiation from measurements of temperature, humidity, and precipitation," *Agricultural and Forest Meteorology*, vol. 93, no. 4, pp. 211–228, 1999 (cit. on p. 10).
- [36] K. Huang, X. Lee, B. Stone Jr, J. Kniewel, M. L. Bell and K. C. Seto, "Persistent increases in nighttime heat stress from urban expansion despite heat island mitigation," *Journal of Geophysical Research: Atmospheres*, vol. 126, no. 4, 2021 (cit. on p. 10).
- [37] M. Robitu, M. Musy, C. Inard and D. Groleau, "Modeling the influence of vegetation and water pond on urban microclimate," *Solar Energy*, vol. 80, no. 4, pp. 435–447, 2006. DOI: <https://doi.org/10.1016/j.solener.2005.06.015> (cit. on pp. 11, 17, 18).
- [38] Y. Ko, "Urban form and residential energy use: A review of design principles and research findings," *Journal of Planning Literature*, vol. 28, no. 4, pp. 327–351, 2013 (cit. on p. 11).
- [39] S. Reiter and A. De Herde, "Qualitative and quantitative criteria for comfortable urban public spaces," in *Research in Building Physics*, CRC Press, 2020, pp. 1001–1009 (cit. on p. 12).
- [40] S. Lenzholzer, W. Klemm and C. Vasilikou, "Qualitative methods to explore thermo-spatial perception in outdoor urban spaces," *Urban Climate*, vol. 23, pp. 231–249, 2018. DOI: <https://doi.org/10.1016/j.uclim.2016.10.003> (cit. on p. 12).
- [41] S. G. Tavares, "URBAN COMFORT: Adaptive capacity in post-earthquake Christchurch," Ph.D. dissertation, Lincoln University, 2015 (cit. on p. 12).
- [42] A. Davenport and N Isyumov, "The ground level wind environment in built-up areas," in *Proceedings of Fourth International Conference on Wind Effects on Buildings and Structures*, (Heathrow, UK), Cambridge University Press, 1975, pp. 403–422 (cit. on p. 12).
- [43] T. Lawson and A. Penwarden, "The effects of wind on people in the vicinity of buildings," in *Proceedings of Fourth International Conference on Wind Effects on Buildings and Structures*, (Heathrow, UK), Cambridge University Press, 1975, pp. 605–622 (cit. on p. 12).
- [44] T. Lawson, "The wind content of the built environment," *Journal of Wind Engineering and Industrial Aerodynamics*, vol. 3, no. 2-3, pp. 93–105, 1978. DOI: [https://doi.org/10.1016/0167-6105\(78\)90002-8](https://doi.org/10.1016/0167-6105(78)90002-8) (cit. on p. 12).

- [45] T. Lawson, “The determination of the wind environment of a building complex before construction,” *Department of Aerospace Engineering, University of Bristol, Report Number TVL*, vol. 9025, 1990 (cit. on p. 12).
- [46] NEN, “Wind comfort en wind danger in the built environment,” NEN, The Netherlands, Standard, Feb. 2006 (cit. on p. 12).
- [47] D. Lai, Z. Lian, W. Liu *et al.*, “A comprehensive review of thermal comfort studies in urban open spaces,” *Science of the Total Environment*, vol. 742, p. 140 092, 2020. DOI: <https://doi.org/10.1016/j.scitotenv.2020.140092> (cit. on p. 13).
- [48] G. M. Budd, “Wet-bulb globe temperature (wbgt)—its history and its limitations,” *Journal of Science and Medicine in Sport*, vol. 11, no. 1, pp. 20–32, 2008. DOI: <https://doi.org/10.1016/j.jsams.2007.07.003> (cit. on p. 13).
- [49] P. Bröde, D. Fiala, K. Błażejczyk *et al.*, “Deriving the operational procedure for the universal thermal climate index (utci),” *International Journal of Biometeorology*, vol. 56, no. 3, pp. 481–494, 2012. DOI: <https://doi.org/10.1007/s00484-011-0454-1> (cit. on p. 13).
- [50] P. Höppe, “The physiological equivalent temperature—a universal index for the biometeorological assessment of the thermal environment,” *International Journal of Biometeorology*, vol. 43, no. 2, pp. 71–75, 1999. DOI: <https://doi.org/10.1007/s004840050118> (cit. on p. 13).
- [51] C García-Sánchez, J van Beeck and C Górlé, “Predictive large eddy simulations for urban flows: Challenges and opportunities,” *Building and Environment*, vol. 139, pp. 146–156, 2018. DOI: <https://doi.org/10.1016/j.buildenv.2018.05.007> (cit. on p. 17).
- [52] C García-Sánchez, G Van Tendeloo and C Górlé, “Quantifying inflow uncertainties in rans simulations of urban pollutant dispersion,” *Atmospheric Environment*, vol. 161, pp. 263–273, 2017. DOI: <https://doi.org/10.1016/j.atmosenv.2017.04.019> (cit. on p. 17).
- [53] R Yoshie, A. Mochida, Y Tominaga *et al.*, “Cooperative project for CFD prediction of pedestrian wind environment in the Architectural Institute of Japan,” *Journal of Wind Engineering and Industrial Aerodynamics*, vol. 95, no. 9-11, pp. 1551–1578, 2007. DOI: <https://doi.org/10.1016/j.jweia.2007.02.023> (cit. on p. 18).
- [54] B. Blocken, W. Janssen and T. van Hooff, “CFD simulation for pedestrian wind comfort and wind safety in urban areas: General decision framework and case study for the eindhoven university campus,” *Environmental Modelling & Software*, vol. 30, pp. 15–34, 2012. DOI: <https://doi.org/10.1016/j.envsoft.2011.11.009> (cit. on p. 18).
- [55] J. Amorim, V Rodrigues, R Tavares, J Valente and C Borrego, “CFD modelling of the aerodynamic effect of trees on urban air pollution dispersion,” *Science of the Total Environment*, vol. 461, pp. 541–551, 2013. DOI: <https://doi.org/10.1016/j.scitotenv.2013.05.031> (cit. on p. 18).

- [56] H. Huang, R. Ooka, H. Chen, S. Kato, T. Takahashi and T. Watanabe, "CFD analysis on traffic-induced air pollutant dispersion under non-isothermal condition in a complex urban area in winter," *Journal of Wind Engineering and Industrial Aerodynamics*, vol. 96, no. 10-11, pp. 1774–1788, 2008. DOI: <https://doi.org/10.1016/j.jweia.2008.02.010> (cit. on p. 18).
- [57] G. Stavrakakis, E Tzanaki, V. Genetzaki, G Anagnostakis, G Galetakis and E Grigorakis, "A computational methodology for effective bioclimatic-design applications in the urban environment," *Sustainable Cities and Society*, vol. 4, pp. 41–57, 2012. DOI: <https://doi.org/10.1016/j.scs.2012.05.002> (cit. on p. 18).
- [58] N. Y. Tong and D. Y. Leung, "Effects of building aspect ratio, diurnal heating scenario, and wind speed on reactive pollutant dispersion in urban street canyons," *Journal of Environmental Sciences*, vol. 24, no. 12, pp. 2091–2103, 2012. DOI: [https://doi.org/10.1016/S1001-0742\(11\)60971-6](https://doi.org/10.1016/S1001-0742(11)60971-6) (cit. on p. 18).
- [59] Y. Fan, Y. Li, A. Bejan, Y. Wang and X. Yang, "Horizontal extent of the urban heat dome flow," *Scientific reports*, vol. 7, no. 1, pp. 1–10, 2017. DOI: <https://doi.org/10.1038/s41598-017-09917-4> (cit. on p. 18).
- [60] C. Gromke, B. Blocken, W. Janssen, B. Merema, T. van Hooff and H. Timmermans, "CFD analysis of transpirational cooling by vegetation: Case study for specific meteorological conditions during a heat wave in arnhem, netherlands," *Building and Environment*, vol. 83, pp. 11–26, 2015. DOI: <https://doi.org/10.1016/j.buildenv.2014.04.022> (cit. on p. 18).
- [61] P. Gkatsopoulos, "A methodology for calculating cooling from vegetation evapotranspiration for use in urban space microclimate simulations," *Procedia Environmental Sciences*, vol. 38, pp. 477–484, 2017. DOI: <https://doi.org/10.1016/j.proenv.2017.03.139> (cit. on p. 18).
- [62] R. Buccolieri, J.-L. Santiago, E. Rivas and B. Sanchez, "Review on urban tree modelling in CFD simulations: Aerodynamic, deposition and thermal effects," *Urban Forestry & Urban Greening*, vol. 31, pp. 212–220, 2018. DOI: <https://doi.org/10.1016/j.ufug.2018.03.003> (cit. on p. 18).
- [63] J. P. Van Doormaal and G. D. Raithby, "Enhancements of the simple method for predicting incompressible fluid flows," *Numerical heat transfer*, vol. 7, no. 2, pp. 147–163, 1984. DOI: <https://doi.org/10.1080/01495728408961817> (cit. on p. 19).
- [64] J. Van Doormaal and G. Raithby, "Enhancements of the SIMPLE method for predicting incompressible fluid flows," *Numerical Heat Transfer*, vol. 7, no. 2, p. 147, 1984. DOI: <https://doi.org/10.1080/01495728408961817> (cit. on p. 19).
- [65] C. M. Rhie and W.-L. Chow, "Numerical study of the turbulent flow past an airfoil with trailing edge separation," *AIAA journal*, vol. 21, no. 11, pp. 1525–1532, 1983. DOI: <https://doi.org/10.2514/3.8284> (cit. on p. 19).

- [66] C. S. Peskin, “The fluid dynamics of heart valves: Experimental, theoretical, and computational methods,” *Annual review of fluid mechanics*, vol. 14, no. 1, pp. 235–259, 1982. DOI: <https://doi.org/10.1146/annurev.fl.14.010182.001315> (cit. on p. 19).
- [67] W.-P. Breugem, “A second-order accurate immersed boundary method for fully resolved simulations of particle-laden flows,” *Journal of Computational Physics*, vol. 231, no. 13, pp. 4469–4498, 2012. DOI: <https://doi.org/10.1016/j.jcp.2012.02.026> (cit. on p. 19).
- [68] A. Mark and B. G. van Wachem, “Derivation and validation of a novel implicit second-order accurate immersed boundary method,” *Journal of Computational Physics*, vol. 227, no. 13, pp. 6660–6680, 2008. DOI: <https://doi.org/10.1016/j.jcp.2008.03.031> (cit. on p. 20).
- [69] S. Allmaras, F. Johnson and P. Spalart, “Modifications and non-linear in the boundary layer. several validation cases clarifications for the implementation of the Spalart-Allmaras in both two and three dimensions were provided, exhibit- turbulence model,” *Seventh International Conference on Computational Fluid Dynamics (ICCFD7)*, 2012 (cit. on p. 21).
- [70] B. E. Launder and D. B. Spalding, “The numerical computation of turbulent flows,” in *Numerical Prediction of Flow, Heat Transfer, Turbulence and Combustion*, Elsevier, 1983, pp. 96–116. DOI: <https://doi.org/10.1016/B978-0-08-030937-8.50016-7> (cit. on p. 21).
- [71] T.-H. Shih, W. Liou, A. Shabbir, Z. Yang and J. Zhu, “A new $k - \epsilon$ eddy viscosity model for high Reynolds number turbulent flows,” *Journal of Computational Physics*, vol. 24, no. 3, pp. 227–238, 1995 (cit. on p. 21).
- [72] F. R. Menter, “Two-equation eddy-viscosity turbulence models for engineering applications,” *AIAA Journal*, vol. 32, no. 8, 1994 (cit. on p. 21).
- [73] F. R. Menter, M. Kuntz and M. R. Langtry, “Ten years of industrial experience with the SST turbulence model,” *Turbulence, Heat and Mass Transfer*, vol. 4, 1994 (cit. on p. 21).
- [74] D. Wilcox, *Turbulence Modeling for CFD*. DCW Industries, 2010 (cit. on p. 21).
- [75] G. Kalitzin, G. Medic, G. Iaccarino and P. Durbin, “Near-wall behavior of RANS turbulence models and implications for wall functions,” *Journal of Computational Physics*, vol. 204, 2005. DOI: <https://doi.org/10.1016/j.jcp.2004.10.018> (cit. on p. 22).
- [76] A. Mark, E. Svenning and F. Edelvik, “An immersed boundary method for simulation of flow with heat transfer,” *International Journal of Heat and Mass Transfer*, vol. 56, no. 1-2, pp. 424–435, 2013. DOI: <https://doi.org/10.1016/j.ijheatmasstransfer.2012.09.010> (cit. on p. 22).

- [77] F. Svelander, G. Kettil, T. Johnson, A. Mark, A. Logg and F. Edelvik, “Robust intersection of structured hexahedral meshes and degenerate triangle meshes with volume fraction applications,” *Numerical Algorithms*, vol. 77, no. 4, pp. 1029–1068, 2018. DOI: <https://doi.org/10.1007/s11075-017-0352-7> (cit. on p. 22).
- [78] T. Andersson, D. Nowak, T. Johnson, A. Mark, F. Edelvik and K.-H. Küfer, “Multiobjective optimization of a heat-sink design using the sandwiching algorithm and an immersed boundary conjugate heat transfer solver,” *Journal of Heat Transfer*, vol. 140, no. 10, 2018. DOI: <https://doi.org/10.1115/1.4040086> (cit. on p. 23).
- [79] B. Aupoix and P. Spalart, “Extensions of the Spalart–Allmaras turbulence model to account for wall roughness,” *International Journal of Heat and Fluid Flow*, vol. 24, no. 4, pp. 454–462, 2003. DOI: [https://doi.org/10.1016/S0142-727X\(03\)00043-2](https://doi.org/10.1016/S0142-727X(03)00043-2) (cit. on p. 23).
- [80] B. Aupoix, “Roughness Corrections for the $k-\omega$ Shear Stress Transport Model: Status and Proposals,” *Journal of Fluids Engineering*, vol. 137, no. 2, Sep. 2014. DOI: <https://doi.org/10.1115/1.4028122> (cit. on p. 23).
- [81] F. Chedevergne, “Analytical wall function including roughness corrections,” *International Journal of Heat and Fluid Flow*, vol. 73, pp. 258–269, 2018. DOI: <https://doi.org/10.1016/j.ijheatfluidflow.2018.08.001> (cit. on p. 23).
- [82] A. G. Davenport, “Rationale for determining design wind velocities,” *Journal of the Structural Division*, vol. 86, no. 5, pp. 39–68, 1960 (cit. on p. 23).
- [83] J. Wieringa, “Updating the davenport roughness classification,” *Journal of Wind Engineering and Industrial Aerodynamics*, vol. 41, no. 1-3, pp. 357–368, 1992. DOI: [https://doi.org/10.1016/0167-6105\(92\)90434-C](https://doi.org/10.1016/0167-6105(92)90434-C) (cit. on p. 23).
- [84] B. Blocken, T. Stathopoulos and J. Carmeliet, “CFD simulation of the atmospheric boundary layer: Wall function problems,” *Atmospheric Environment*, vol. 41, no. 2, pp. 238–252, 2007. DOI: <https://doi.org/10.1016/j.atmosenv.2006.08.019> (cit. on p. 23).
- [85] J. Allegrini, “A wind tunnel study on three-dimensional buoyant flows in street canyons with different roof shapes and building lengths,” *Building and Environment*, vol. 143, pp. 71–88, 2018 (cit. on pp. 25, 29).